On the density of shear transformations in amorphous solids

Lin, J.; Saade, A.; Lerner, E.; Rosso, A.; Wyart, M.

DOI
10.1209/0295-5075/105/26003
Publication date
2014
Document Version
Final published version
Published in
Europhysics Letters

A Letters Journal Exploring the Frontiers of Physics

January 2014

EPL, **105** (2014) 26003 www.epljournal.org
doi: 10.1209/0295-5075/105/26003

On the density of shear transformations in amorphous solids

Jie Lin[1], Alaa Saade[1,3], Edan Lerner[1], Alberto Rosso[2] and Matthieu Wyart[1]

[1] *New York University, Center for Soft Matter Research - 4 Washington Place, New York, NY, 10003, USA*
[2] *Laboratoire de Physique Théorique et Modèles Statistiques (UMR CNRS 8626), Université de Paris-Sud Orsay Cedex, France*
[3] *LPS, ENS - 24 rue Lhomond, 75231 Paris Cedex 05, France*

received 9 October 2013; accepted in final form 13 January 2014
published online 11 February 2014

PACS 63.50.-x – Vibrational states in disordered systems
PACS 63.50.Lm – Glasses and amorphous solids
PACS 45.70.-n – Granular systems

Abstract – We study the stability of amorphous solids, focussing on the distribution $P(x)$ of the local stress increase x that would lead to an instability. We argue that this distribution behaves as $P(x) \sim x^\theta$, where the exponent θ is larger than zero if the elastic interaction between rearranging regions is non-monotonic, and increases with the interaction range. For a class of finite-dimensional models we show that stability implies a lower bound on θ, which is found to lie near saturation. For quadrupolar interactions these models yield $\theta \approx 0.6$ for $d = 2$ and $\theta \approx 0.4$ in $d = 3$ where d is the spatial dimension, accurately capturing previously unresolved observations in atomistic models, both in quasi-static flow and after a fast quench. In addition, we compute the Herschel-Buckley exponent in these models and show that it depends on a subtle choice of dynamical rules, whereas the exponent θ does not.

Dislocations play a key role in controlling plastic flow in crystalline solids. In contrast, the notion of defects is ill-defined in amorphous materials. However, plasticity under shear in these materials occurs via events that are also well localized in space [1–6]. There are thus preferential locations where plastic rearrangements are likely to occur, which we refer to as shear transformations [1], and are central to various proposed descriptions of plasticity [7]. The microscopic nature of these objects is however elusive, and their concentration is thus hard to measure directly [8,9].

Recently, it has been shown [10,11] that the density of soft, non-linear excitations in hard-sphere packings is such that stability toward extensive rearrangements is achieved, but barely so. This result raises the question of how the stability of amorphous solids with smooth interactions is reflected by the distribution of shear transformations $P(x)$, which measures the density of regions that flow plastically if the local stress is incremented by x. Although phenomenological models of plasticity do not consider this possibility, there is indirect evidence that $P(x)$ is not analytical but behaves as $P(x) \sim x^\theta$ [12]: both following a quench and during steady flow, the amount by which the stress can be increased without triggering plastic events in a system of N particles was found to scale in a numerical molecular glass as $N^{-\xi}$ where $\xi < 1$. Assuming that the variables x are independent, this observation would imply that $\theta > 0$ as we shall recall below. However, the hypothesis of independence is inconsistent with observations at the yield stress [12], raising doubts on the inference of θ. Most importantly, what controls this exponent is not known.

In this letter we argue that θ is governed by the interaction between shear transformations, and is such that extensive avalanches of plastic rearrangements are prohibited. θ can be non-zero if the interaction is non-monotonic, *i.e.* is either stabilizing or destabilizing depending on the location, and increases with the interaction range. We extend a previous mean-field, on-lattice model of plasticity [13] to the case of power-law interactions, and show that stability implies a lower bound on θ, which is found to lie near saturation. When more realistic quadrupolar interactions are considered, which are known to characterize the far field effect of a plastic event [5,6], the model yields $\theta \approx 0.6$ for $d = 2$ and $\theta \approx 0.4$ in $d = 3$, and reproduces at a surprising level of accuracy the system size dependence of the strain interval between plastic events observed in atomistic models [12]. Our findings underlines a missing ingredient in the description of plasticity of amorphous solids, and suggests an explanation for puzzling differences between this phenomenon and the depinning transition where an elastic manifold is driven in a random environment.

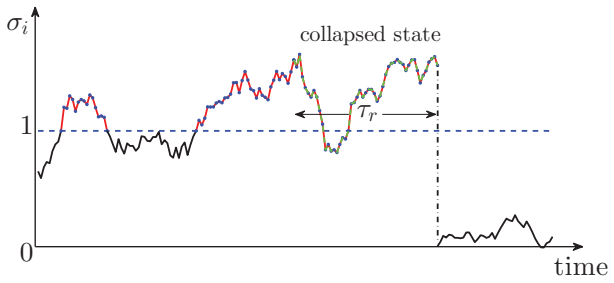

Fig. 1: (Colour on-line) Illustration of a possible trajectory of the local stress σ_i at site i *vs.* time in our model. As time evolves, σ_i fluctuates due to interactions with other sites. During the intervals for which $\sigma_i > \sigma^{th} \equiv 1$ (red line with dots), the site has a probability per unit time $1/\tau_c$ to go into the "collapsed state", marked in the illustration by the dashed red-green line. Sites are not stabilized while in the collapsed state, even if $\sigma_i < 1$ during that time. After a mean duration τ_r, the site leaves the collapsed state, the local stress σ_i is set to zero, and the local stresses σ_j in other sites $j \neq i$ are updated according to the interaction law $\sigma_j \leftarrow \sigma_j + \mathcal{G}(\vec{r}_i - \vec{r}_j)$.

We focus on athermal amorphous materials under simple shear, and work at constant shear stress σ. We consider cellular automaton models which are known to capture the critical behavior of the depinning transition [14] and have been used to study plastic flow [13,15–18]. The sample is decomposed into sites labelled by i, each carrying a scalar shear stress σ_i (the tensorial nature of the stress is neglected). A site represents a few particles. The applied shear stress is $\sigma = \frac{1}{N}\sum_i \sigma_i$. Each site is described by a local yield stress beyond which plasticity occurs. For simplicity we assume that this threshold σ^{th} is independent of position, and in what follows σ^{th} defines our unit of stress. Two time scales characterize the dynamics of our model. If $\sigma_i > \sigma^{th}$, the site i is mechanically unstable, and has a probability per unit time $1/\tau_c$ to rearrange plastically. As illustrated in fig. 1, the interactions with other sites (to be specified in the following) can bring back the local stress below threshold ($\sigma_i < \sigma^{th} \equiv 1$) before it had time to yield. If this happens, the site becomes stable again. Physically, τ_c is the characteristic time to relax locally toward a new local minimum of potential energy, and is thus a vibrational time (of order of the inverse Debye frequency). In principle τ_c should depend on how unstable the site is (*i.e.* on $\sigma_i - \sigma^{th}$), for simplicity we neglect this dependence. Such a plastic event affects the stress in the rest of the system, with a delay associated to elastic propagation. We neglect the dependence of this delay on the distance from the plastic event, and choose the delay times to be exponentially distributed with mean τ_r. For conveniency, we refer to sites that have undergone a plastic rearrangement, but have not yet affected other sites (sites remain in this state for a typical duration τ_r) as being in the "collapsed state". While in the collapsed state, sites cannot be restablized, even if their local stress drops below the threshold. The return of a site from the collapsed state to mechanical stability is accompanied by the following changes in the local stresses:

$$\sigma_i \leftarrow 0, \tag{1}$$

$$\sigma_j \leftarrow \sigma_j + \mathcal{G}(\vec{r}_i - \vec{r}_j). \tag{2}$$

In simple depinning models, $\mathcal{G}$ is strictly positive and the interaction is said to be monotonic. We focus here on non-monotonic interactions for which the sign of $\mathcal{G}$ varies. In this case if $\tau_c > 0$, unstable sites can be re-stabilized by other plastic events. Such models predict the existence of a yield stress, and as we shall demonstrate are consistent with the Herschel-Bulkley (HB) relation:

$$\dot{\gamma} \sim (\sigma - \sigma_c)^{\beta}, \tag{3}$$

where the strain rate $\dot{\gamma}$ is defined as the number of collapses per unit time. In numerical simulations finite-size fluctuations can stop the dynamics even if $\sigma > \sigma_c$. When this happens we give small random kicks to every site (while conserving the total stress constant) until a new site becomes unstable. This method enables us to reach the steady state when $\sigma > \sigma_c$ and to study avalanche dynamics at σ_c.

We denote the distance to the yield stress of the site i by $x_i \equiv 1 - \sigma_i$. In principle x_i can be measured experimentally or numerically by observing how much additional stress can be locally applied to site i before plasticity occurs. Our goal is to understand how the distribution $P(x)$ depends on the interaction $\mathcal{G}$. We introduce the decomposition $P(x) = P_1(x) + P_2(x)$ where $P_2(x)$ is the distribution of collapsed sites, and $P_1(x)$ is the distribution of the rest of the sites.

We first consider a solvable mean-field model where it is assumed that a plastic event leads to random kicks of stress whose magnitude does not depend on position:

$$\mathcal{G}_{\rm mean}(\vec{r}_i - \vec{r}_j) = \frac{\eta_j}{\sqrt{N}} + \frac{\tilde{\eta}}{N}, \tag{4}$$

where the η_j are independent variables in space, and are uncorrelated from one plastic event to the next. They are uniformly distributed in $[-\eta_0, \eta_0]$, and η_0 does not depend on N to ensure the existence of a thermodynamic limit. $\tilde{\eta}$ is chosen at each collapse event to ensure that the total stress is conserved, and thus depends on the random variables η_j of that event. This model is a variation of that of Hebraud and Lequeux [13], and we briefly recall how to solve it.

In the thermodynamic limit eq. (4) implies a Fokker-Planck equation for active sites:

$$\frac{\partial P_1(x)}{\partial t} = \dot{\gamma}\Big(D\frac{\partial^2 P_1(x)}{\partial x^2} + \lambda\frac{\partial P_1(x)}{\partial x} + \delta(x-1)\Big) - \Theta(-x)\frac{P_1(x)}{\tau_c} \tag{5}$$

and an equation of similar form for $P_2(x)$ (see appendix). $D \equiv \eta_0^2/6$ represents the diffusion constant of the local

stress (and is unrelated to the particle diffusion constant), coming from the random kicks of other collapsing sites. λ is a Lagrange parameter that constrains the average stress, and is chosen such that $\int xP(x)\mathrm{d}x = 1-\sigma$. It results from the second term on the RHS of eq. (4). The δ-function term corresponds to the flux of reinserted sites at $\sigma = 0$, equivalent to $x = 1$. The last term in eq. (5) corresponds to the flux of unstable sites that collapse, and $\Theta(x)$ is the Heaviside function. Equation (5), together with a similar equation for $P_2(x)$, are closed. We find (see appendix) that no stationary solution with $\dot\gamma > 0$ exists for $\sigma < \sigma_c = 1/2 - D$. The critical distribution, at $\lambda = 1$ ($\sigma = \sigma_c \implies \dot\gamma = 0$) is independent of τ_c and τ_r and follows:

$$\begin{aligned} P_c(x) &= 0, & x &< 0, \\ P_c(x) &= 1 - \exp(-x/D), & 0 &< x < 1, \\ P_c(x) &= (\exp(1/D) - 1), \exp(-x/D), & x &> 1. \end{aligned} \quad (6)$$

Taking the mean, one obtains $x_c = D + \frac{1}{2}$, implying for the yield stress $\sigma_c = \frac{1}{2} - D$. Equation (6) satisfies $P_c(x) \sim x$ for small x, which means that in mean field, $\theta = 1$. This linear density of nearly unstable regions has a simple explanation: the stress in each site follows a diffusion equation. In the limit of small strain rate the instability threshold at $x = 0$ becomes an absorbing boundary condition. In contrast, for monotonic problems such as pinned elastic interfaces, the distance to a local instability x is always decreasing in time and $P(x)$ thus cannot vanish at $x = 0$. Solving this mean-field model at finite strain rate, we find at first order in $\dot\gamma$:

$$\sigma - \sigma_c = \left(\frac{1}{2}+D\right)\sqrt{D\tau_c}\dot\gamma^{1/2} + \left[\tau_r\left(\frac{1}{2}+2D\right) + \frac{\tau_c}{4} + (1-D)D\tau_c\right]\dot\gamma. \quad (7)$$

We thus see that if $\tau_c \neq 0$, $\sigma - \sigma_c \sim \dot\gamma^{1/2}$, corresponding to $\beta = 2$ in eq. (3), as also obtained in the model of [13]. However, if $\tau_c = 0$, $\sigma - \sigma_c \sim \dot\gamma$, corresponding to $\beta = 1$. Thus the models with $\tau_c = 0$ and $\tau_c > 0$ display different rheological properties. This situation does not occur in depinning with monotonic interactions, for which the details of the model dynamics are irrelevant [19]. Although one expects generically that in physical situations $\tau_c > 0$, including the case $\tau_c = 0$ is informative, as it allows one to test which properties are robust toward changes of dynamical rules. Thus in what follows we consider two sets of parameters:

1) model A, with $\tau_r = 0$ and $\tau_c = 1$;

2) model B, with $\tau_r = 1$ and $\tau_c = 0$.

Equation (7) is confirmed numerically in fig. 2 for both models. Despite the notable difference between the dynamics of models A and B, $P(x)$ at the critical stress is independent of the choice of dynamics. This supports that

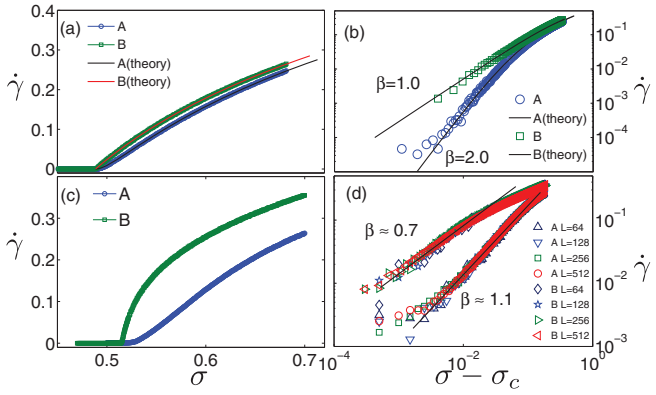

Fig. 2: (Colour on-line) $\dot\gamma$ *vs.* σ for models A ($\tau_c = 1$, $\tau_r = 0$) and B ($\tau_c = 0$, $\tau_r = 1$). Top panels: mean-field interactions with $D = 1/6$ on (a) linear and (b) log-log scales. Bottom panels: quadrupole interactions for $d = 2$ on (c) linear and (d) log-log scales. The fits give $\beta \approx 1.1$, $\sigma_c \approx 0.52$ for model A and $\beta \approx 0.7$, $\sigma_c \approx 0.515$ for model B.

the class of models we consider should yield correct values for θ. Moreover, we find at σ_c that the avalanches distribution $\rho(S)$, where S is the number of plastic events, follows $\rho(S) \sim 1/S^\tau$ with $\tau \approx 1.5$ independently of the choice of dynamics, as shown in fig. 3. This result is consistent with mean-field depinning [19] and the ABBM model [20].

To study finite-dimensional effects, we now consider interactions decaying with distance, of the form

$$\mathcal{G}(\vec r_i - \vec r_j) = \frac{\eta_j}{r_{ij}^\alpha} + \eta_1, \quad (8)$$

where $\eta_j \in [-\eta, \eta]$ is a random variable uniformly distributed, and η_1 is again a global shift to keep the average stress constant. To ensure that the random kicks of eq. (8) have a finite effect on the stress in the thermodynamic limit, the coefficient η must be such that $\int_1^L \frac{\eta^2}{r^{2\alpha}}\mathrm{d}^d r \sim 1$ where d is the spatial dimension and L the linear system size. We get $\eta \sim L^{\alpha - d/2}$ for $\alpha < d/2$, $\eta \sim 1/\sqrt{\ln L}$ for $\alpha = d/2$ and $\eta \sim 1$ for $\alpha > d/2$.

Computing θ is now a much harder problem. However, we now show that stability implies a bound on this exponent. We denote by m the average number of plastic events that are triggered if one single event at the origin takes place. We assume that the distribution $P(x)$ satisfies $P(x) \sim x^\theta$. A site at a distance r experiences a kick which contains the term η_1 of order $1/N$ that stems from stress conservation, and a term η/r^α, which is destabilizing or stabilizing with probability 1/2. The term $\eta_1 \sim 1/N$ will destabilize the site with a probability $p_1 \sim P(x < 1/N) \sim N^{-(1+\theta)}$, so that overall in the entire system this will trigger of the order of $N^{-\theta}$ events, which is negligible as long as $\theta > 0$. The probability $p_2(r)$ that the term η/r^α destabilizes the site is of order $p_2(r) = P(x \leq \eta/r^\alpha)/2 \sim \eta^{\theta+1}/r^{\alpha(\theta+1)}$. Integrating over

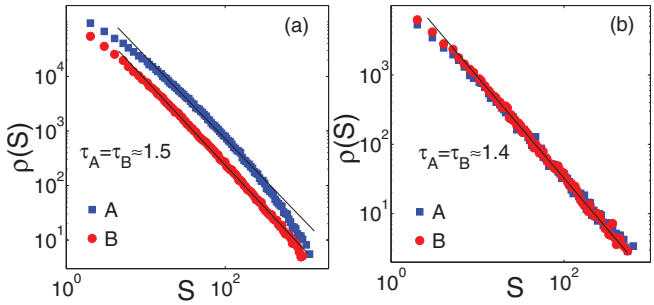

Fig. 3: (Colour on-line) Distribution of avalanches size for (a) mean-field interaction and (b) quadrupole interactions.

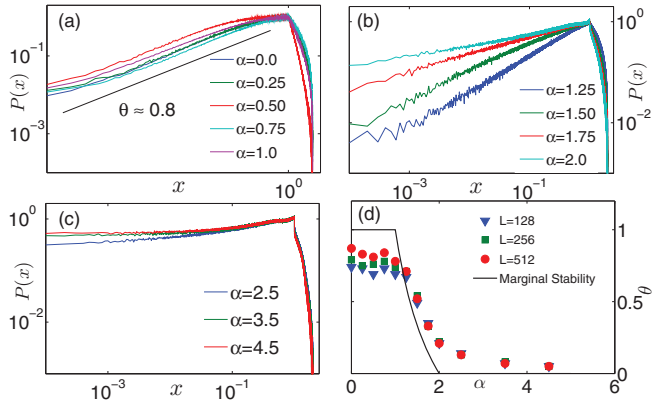

Fig. 4: (Colour on-line) $P(x)$ *vs.* x for $d = 2$ systems with the power-law interactions of eq. (8): (a) when $\alpha \leq 1$, $\theta \geq 0.8$; (b) when $1 < \alpha \leq 2$, θ decreases as α increases; (c) when $\alpha > 2$, $\theta \approx 0$. (d) θ *vs.* α obtained in our simulations and compared with the theoretical lower bound of eq. (11).

all sites we get

$$m \sim \eta^{\theta+1} \int_1^L \frac{\mathrm{d}r}{r^{\alpha(\theta+1)+1-d}} \sim \eta^{\theta+1} L^{d-\alpha(\theta+1)} \sim L^{\nu}, \quad (9)$$

where the exponent ν can be computed from the dependence of η with L. Stability toward run-away avalanches requires $\nu \leq 0$, which finally leads to

$$\begin{aligned} \theta &\geq 1, && \text{if } d \geq 2\alpha, \\ \theta &\geq \frac{d}{\alpha} - 1, && \text{if } d/2 \leq \alpha \leq d, \\ \theta &\geq 0, && \text{if } \alpha > d. \end{aligned} \quad (10)$$

This prediction is tested in fig. 4, where $P(x)$ is shown for various interaction range α in two dimensions, from which the exponent θ is extracted. Figure 4(d) shows the comparison between the measurement and the stability bound. For $\alpha < 1$ the bound appears slightly violated, but less and less so for larger system sizes, supporting that $\theta = 1$, as we predicted exactly for $\alpha = 0$. For larger α, θ is found to lie close to the bound but systematically above, although our data cannot rule out saturation. Our analysis thus implies that the range of interaction is a key determinant of $P(x)$ and θ, and that for this class of models, systems lie close to marginal stability.

Finally, we consider the more realistic case where the interaction is not random, but quadrupolar in the far field [6,21]. Our model then belongs to the class of elasto-plastic models [16–18,22]. In two dimensions for a simple shear along the x-axis one has for an infinite system $\mathcal{G}(r) = \frac{\cos 4\phi}{r^2}$, where ϕ is the angle made with the x-axis. Periodic boundary conditions can be implemented using the Fourier representation, $\mathcal{G}(k_x, k_y) = k_x^2 k_y^2/k^4$, and the discrete wave vectors, $k_x = 2\pi n_x/L$,$k_y = 2\pi n_y/L$. This interaction can be computed also in $d = 3$ where it decays as $\mathcal{G}(r) \sim 1/r^3$.

To our knowledge the exponent β of eq. (3) has not been computed for such models. Our results are shown in fig. 2 bottom for dynamics A and B, and are well-captured by the HB law with $\beta_{\mathrm{A}} \approx 1.1$ and $\beta_{\mathrm{B}} \approx 0.7$. We also compute the avalanche exponent and find $\tau \approx 1.42$ in both dynamics, again close to the mean-field value 1.5 in agreement with [16] but somewhat larger than [22], as shown in fig. 3. Note that in these numerics the initial condition is chosen such that the stress averages on each line or column is identical, a condition that remains satisfied as the system evolves. This choice is physically sound (as it enforces force balance on each slab of the system), and turns out to greatly reduce finite-size effects.

One central result concerns the density of excitations $P(x)$. We measure this quantity in two situations: i) at the yield stress σ_c, in the steady state, ii) at $\sigma = 0$ after a "quench" which mimics the behavior that would occur if the temperature was suddenly set to zero in a liquid. In the latter case the *initial* local stress, σ_i, are drawn from a symmetric distribution $Q_0(\sigma_i)$, so that $\sigma = 0$. We find that the results do not depend on the variance of $Q_0(\sigma_i)$ as long as it is larger than the yield stress, here we choose $\langle \sigma^2 \rangle = 1.2$. In this condition the system is unstable because many sites with $|\sigma_i| > 1$ can collapse and trigger other rearrangements. This dynamics stops when $|\sigma_i| < 1$ on all sites. Our results are shown in fig. 5. We find that $\theta \approx 0.6$ in two dimensions and $\theta \approx 0.4$ in three dimensions, both at σ_c and after the quench at $\sigma = 0$.

Can such a simple model, that neglects in particular the tensorial nature of stress, capture essential aspects of the glassy dynamics that occurs during an isotropic quench? To test this hypothesis we compare our results with the atomistic simulations of [12]. $P(x)$ is not available directly, but the statistics of $x_{\min}$ can be obtained accurately by considering the minimal increment of strain, or stress, required to generate a plastic event. It is found that $\langle x_{\min} \rangle \sim N^{-\xi}$ with $\xi \approx 0.62$ after a quench, and $\xi \approx 2/3$ at the yield stress, with no clear dependence on the dimension. Our measurements of the exponent ξ are shown in fig. 6, and are remarkably similar to these observations, as we find $\xi \approx 0.63$ in $d = 2$ and $\xi \approx 0.71$ in $d = 3$ both after a quench at $\sigma = 0$ or in the steady state at σ_c. The exponent ξ can be related to θ if one assumes

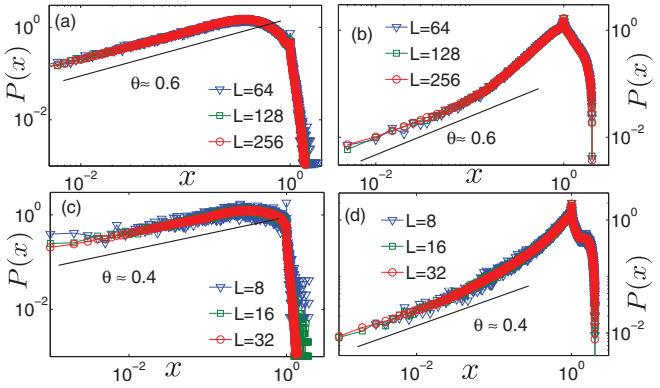

Fig. 5: (Colour on-line) $P(x)$ *vs.* x (a) for $d = 2$ at the critical stress, (b) for $d = 2$ after a fast quench (c) for $d = 3$ at the critical stress and (d) for $d = 3$ after a fast quench. Results are shown for model A, and are identical for model B.

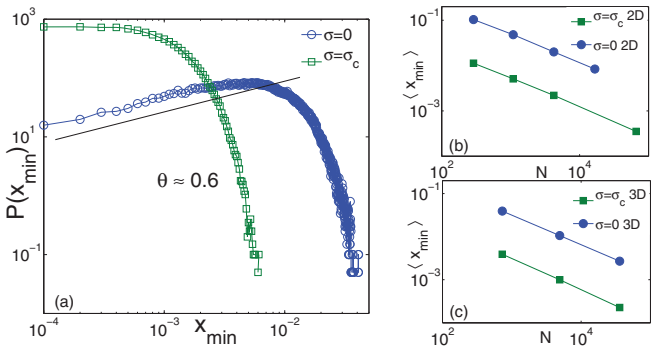

Fig. 6: (Colour on-line) (a) Distribution of the most unstable site $P(x_{\min})$ at σ_c (green squares) and after a rapid quench, at $\sigma = 0$ (blue circles) for $d = 2$. (b), (c): evolution of $\langle x_{\min}\rangle$ *vs.* N indicating a power-law regime $\langle x_{\min}\rangle \sim N^{-\xi}$ with $\xi \approx 0.63$ in $d = 2$ and $\xi \approx 0.71$ in $d = 3$ both for σ_c and the rapid quench.

the independence of the variables x_i:

$$\int_0^{\langle x_{\min}\rangle} \mathrm{d}x\, P(x) \sim \frac{1}{N} \rightarrow \langle x_{\min}\rangle \sim N^{-\frac{1}{\theta+1}} \qquad (11)$$

leading to $\theta = 1/\xi - 1$, a relationship satisfied in our data. The independence assumption also implies a specific form for the distribution of the most unstable site at small argument $P(x_{\min}) \sim x_{\min}^{\theta}$, which is indeed observed in [12] for quenched systems, but not in quasi-static flow, where $P(x_{\min}) \sim x_{\min}^{0}$ was found. Our measurements of $P(x_{\min})$ shown in fig. 6 are strikingly similar to [12], and display precisely these features, supporting the validity of our approach. Our finding that the relationship $\theta = 1/\xi - 1$ holds despite that the lack of strict independence indicates that θ can in principle be extracted from size effects and eq. (11), and may thus be accessible experimentally.

Conclusion. – The phenomenology of the depinning transition [19,23] of an elastic interface is very similar to that of the much less understood yield stress transition [16,22]: there is a critical force F_c where the dynamics also consists of power-law avalanches. At larger forces, the velocity follows $V \sim (F - F_c)^{\beta}$, a form equivalent to the HB relation. There are several important differences however. First, for depinning $\beta \leq 1$ ($\beta = 1$ is the mean-field result), whereas yield stress materials generally display $\beta > 1$. Typical values in the range $\beta \in [2, 3]$ have been found in experiments on two-dimensional sheared foams [24], emulsions [25], and in numerical simulations in two dimensions [26,27]. Here we have shown that models where unstable sites can be re-stabilized, which occurs for non-monotonic interactions and $\tau_c > 0$, can indeed present $\beta > 1$. Our best estimate is $\beta \approx 1.1$. More work is needed, however, to test if this value is affected by our approximations that τ_r is independent of the distance from the plastic event, and that τ_c does not depend on how unstable a site is. Second, in depinning the number of avalanches triggered when F is slightly increased below F_c is extensive and not singular near the transition. This fact allows one to obtain the exponent τ characterizing avalanches [14,28]. Near the yield stress transition, atomistic simulations [29] support that this hypothesis does not hold. We interpret that difference as stemming from the fact that $\theta = 0$ for depinning, whereas $\theta > 0$ for the yielding transition, implying an anomalous relationship between stress increase and number of avalanches triggered.

It would be very interesting to extend this work to finite temperature. Concerning the yielding transition, one may ask if the distribution $P(x)$ remains qualitatively unchanged at finite temperature, or alternatively if a gap appears at small argument. It is indeed possible that below some temperature dependent $x^*(T)$, $P(x)$ is very small, since a nearly unstable site can relax via thermal activation. Concerning the glass transition, the observation that $P(x)$ is singular with the same exponent θ following an isotropic quench suggests that the STZ and their elastic interactions play a role near the glass transition where the system becomes solid and the dynamics stops. This view is supported by recent measurements of strain correlation near the glass transition showing the quadripolar symmetry of the STZ [21]. Further support comes from a recent model emphasizing the role of elastic interactions in thermally activated rearrangements which can rationalize the known relationship between fragility and elasticity in liquids [30].

Overall, our results show that the stability of amorphous solids toward plastic rearrangements is characterized by an exponent θ, which results from the non-monotonic and long-range nature of the interactions between rearranging regions. The presence of this exponent has been overlooked in existing phenomenological models of plasticity, and is expected to affect scaling relations near the yielding transition. This point of view rationalizes some differences between that transition and the much better understood depinning phenomenon, and may thus facilitate the transfer of knowledge between these fields.

* * *

It is a pleasure to thank G. Düring, Le Yan, and Eric DeGiuli for comments on the manuscript and D. Fisher for discussions. This work has been supported by the Sloan Fellowship, NSF CBET-1236378, NSF DMR-1105387, and Petroleum Research Fund #52031-DNI9. This work was also supported partially by the MRSEC Program of the National Science Foundation under Award Number DMR-0820341, and the hospitality of the Aspen Center for Physics.

Appendix. – We give here a few more details about the solution of the mean-field case, eq. (7) in the main text. We write the distribution $P(x)$ as $P(x) = P_1(x) + P_2(x)$, where $P_1(x)$ is the distribution of stable ($x > 0$) and mechanically unstable ($x < 0$) sites, and $P_2(x)$ is the distribution of collapsed sites. In the thermodynamic limit, P_1 and P_2 satisfy the Fokker-Planck equations

$$\frac{\partial P_1(x)}{\partial t} = \dot\gamma\left(D\frac{\partial^2 P_1(x)}{\partial x^2}+\lambda\frac{\partial P_1(x)}{\partial x}+\delta(x-1)\right)-\theta(-x)\frac{P_1(x)}{\tau_c}, \quad \text{(A.1)}$$

$$\frac{\partial P_2(x)}{\partial t} = \dot\gamma\left(D\frac{\partial^2 P_2(x)}{\partial x^2}+\lambda\frac{\partial P_2(x)}{\partial x}\right)+\theta(-x)\frac{P_1(x)}{\tau_c}-\frac{P_2(x)}{\tau_r}. \quad \text{(A.2)}$$

In the stationary limit, these two equations imply, by taking the integral of (A.1) and (A.2), the following conservation law:

$$\dot\gamma = \frac{\int_{-\infty}^{\infty} P_2(x)\mathrm{d}x}{\tau_r} = \frac{\int_{-\infty}^{0} P_1(x)\mathrm{d}x}{\tau_c}. \quad \text{(A.3)}$$

This equality simply states that in a stationary state, the flux of a collapsing site is equal to the flux of sites that become stabilized again. Solving (A.1) gives P_1 up to a constant, which we can then determine thanks to (A.3), using the normalization of the complete distribution P. We find the critical value $\lambda_c = 1$ above which there exists a stationary solution with $\dot\gamma > 0$. The same eq. (A.3) allows to solve for $\dot\gamma$ as a function of $\lambda - \lambda_c$. Expanding for $\lambda \simeq \lambda_c$ gives

$$\dot\gamma = \frac{(\lambda-\lambda_c)^2}{D\tau_c} - \frac{(\tau_c+2\tau_r)(\lambda-\lambda_c)^3}{D^2\tau_c^2} + O(\lambda-\lambda_c)^4. \quad \text{(A.4)}$$

We then have to relate $\lambda - \lambda_c$ and $\sigma - \sigma_c$, which is done using that $\int_{-\infty}^{+\infty} xP(x)\mathrm{d}x = 1 - \sigma$. Multiplying (A.2) by x and integration by parts yields

$$\int_{-\infty}^{+\infty} xP_2(x)\mathrm{d}x = \frac{\tau_r}{D\tau_c}(\lambda_c - \lambda)^3 \quad \text{(A.5)}$$

and because we have already computed P_1, we can compute the expansion of $\sigma - \sigma_c$ in terms of $\lambda - \lambda_c$. A few straightforward computations finally yield eq. (7) of the main text.

REFERENCES

[1] Argon A., *Acta Metall.*, **27** (1979) 47.
[2] Schall P., Weitz D. A. and Spaepen F., *Science*, **318** (2007) 1895.
[3] Amon A., Nguyen V. B., Bruand A., Crassous J. and Clément E., *Phys. Rev. Lett.*, **108** (2012) 135502.
[4] Huang P. Y., Kurasch S., Alden J. S., Shekhawat A., Alemi A. A., McEuen P. L., Sethna J. P., Kaiser U. and Muller D. A., *Science*, **342** (2013) 224.
[5] Maloney C. E. and Lemaitre A., *Phys. Rev. E*, **74** (2006) 016118.
[6] Picard G., Ajdari A., Lequeux F. and Bocquet L., *Eur. Phys. J. E*, **15** (2004) 371.
[7] Falk M. L. and Langer J. S., *Phys. Rev. E*, **57** (1998) 7192.
[8] Rodney D. and Schuh C., *Phys. Rev. Lett.*, **102** (2009) 235503.
[9] Manning M. L. and Liu A. J., *Phys. Rev. Lett.*, **107** (2011) 108302.
[10] Wyart M., *Phys. Rev. Lett.*, **109** (2012) 125502.
[11] Lerner E., Düring G. and Wyart M., *Soft Matter*, **9** (2013) 8252.
[12] Karmakar S., Lerner E. and Procaccia I., *Phys. Rev. E*, **82** (2010) 055103.
[13] Hébraud P. and Lequeux F., *Phys. Rev. Lett.*, **81** (1998) 2934.
[14] Aragón L. E., Jagla E. A. and Rosso A., *Phys. Rev. E*, **85** (2012) 046112.
[15] Baret J.-C., Vandembroucq D. and Roux S., *Phys. Rev. Lett.*, **89** (2002) 195506.
[16] Zaiser M., *Adv. Phys.*, **55** (2006) 185.
[17] Bocquet L., Colin A. and Ajdari A., *Phys. Rev. Lett.*, **103** (2009) 036001.
[18] Martens K., Bocquet L. and Barrat J.-L., *Soft Matter*, **8** (2012) 4197.
[19] Fisher D. S., *Phys. Rep.*, **301** (1998) 113.
[20] Alessandro B., Beatrice C., Bertotti G. and Montorsi A., *J. Appl. Phys.*, **68** (1990) 2901.
[21] Chattoraj J. and Lemaitre A., *Phys. Rev. Lett.*, **111** (2013) 066001.
[22] Talamali M., Petäjä V., Vandembroucq D. and Roux S., *Phys. Rev. E*, **84** (2011) 016115.
[23] Le Doussal P., Wiese K. J. and Chauve P., *Phys. Rev. B*, **66** (2002) 174201.
[24] Möbius M. E., Katgert G. and van Hecke M., *EPL*, **90** (2010) 44003.
[25] Bécu L., Manneville S. and Colin A., *Phys. Rev. Lett.*, **96** (2006) 138302.
[26] Olsson P. and Teitel S., *Phys. Rev. Lett.*, **109** (2012) 108001.
[27] Chaudhuri P., Berthier L. and Bocquet L., *Phys. Rev. E*, **85** (2012) 021503.
[28] Narayan O. and Fisher D. S., *Phys. Rev. B*, **48** (1993) 7030.
[29] Salerno K. M., Maloney C. E. and Robbins M. O., *Phys. Rev. Lett.*, **109** (2012) 105703.
[30] Yan L., Düring G. and Wyart M., *Proc. Natl. Acad. Sci. U.S.A.*, **110** (2013) 6307.